Springtime Arctic haze contributions of submicron organic particles from European and Asian combustion sources

Amanda A. Frossard,[1] Patrick M. Shaw,[1] Lynn M. Russell,[1] Jesse H. Kroll,[2,3] Manjula R. Canagaratna,[3] Douglas R. Worsnop,[3] Patricia K. Quinn,[4] and Timothy S. Bates[4]

Received 12 October 2010; revised 27 December 2010; accepted 4 January 2011; published 9 March 2011.

[1] The composition of Arctic aerosol, especially during the springtime Arctic haze, may play an important role in the radiative balance of the Arctic. The contribution of organic components to Arctic haze has only recently been investigated. Because measurements in this region are sparse, little is known about organic particle composition, sources, and concentrations. This study compares springtime measurements in the Arctic regions north of the Atlantic (ICEALOT, 2008) and Pacific (Barrow, Alaska, 2008 and 2009) oceans. The aerosol organic functional group composition from Fourier transform infrared (FTIR) spectroscopy combined with positive matrix factorization (PMF) and elemental tracer analysis indicate that mixed combustion sources account for more than 60% (>0.3 μg m^{-3}) of the submicron organic mass (OM_1) for springtime haze conditions in both regions. Correlations with typical combustion tracers (S, Zn, K, Br, V) provide evidence for the contribution of combustion sources to the Arctic OM_1. However, the two regions are influenced by different urban and industrial centers with different fuel usage. High-sulfur coal burning in northeastern Europe impacts the northern Atlantic Arctic region, while oil burning and forest fires in northeastern Asia and Alaska impact the northern Pacific Arctic region. Quadrupole and High Resolution Aerosol Mass Spectrometry measurements confirm the highly oxygenated nature of the OM_1, with an oxygenated organic aerosol (OOA) spectrum from PMF. High co-emissions of sulfate and organics from coal-burning in northeastern Europe produce significant concentrations of organosulfate functional groups that account for 10% of OM_1 measured by FTIR spectroscopy during ICEALOT. These observations provide preliminary support for a heterogeneous mechanism of organosulfate formation on acidic sulfate particles.

Citation: Frossard, A. A., P. M. Shaw, L. M. Russell, J. H. Kroll, M. R. Canagaratna, D. R. Worsnop, P. K. Quinn, and T. S. Bates (2011), Springtime Arctic haze contributions of submicron organic particles from European and Asian combustion sources, *J. Geophys. Res.*, *116*, D05205, doi:10.1029/2010JD015178.

1. Background

[2] Arctic haze has been studied since it was reported by pilots over 50 years ago [*Greenaway*, 1950; *Mitchell*, 1956]. This haze is comprised mostly of sulfate aerosol, primarily from anthropogenic sources, with small amounts of ammonium, nitrate, dust, organics, and black carbon [*Li and Barrie*, 1993; *Quinn et al.*, 2002]. Significant anthropogenic sulfur (S) emissions exist within the Arctic region [*Hole et al.*, 2009]. On time scales of a few days to weeks, the polar dome isolates the Arctic lower troposphere from warmer regions to the south making northern Europe and northern Russia major contributors to Arctic haze [*Law and Stohl*, 2007]. However, emissions from populated sub-Arctic regions are the most likely cause of the high aerosol particle concentrations in the springtime Arctic, when meridional transport from the midlatitudes to the Arctic intensifies and brings emissions from Eurasia northward [*Carlson*, 1981; *Iversen*, 1984; *Iversen and Joranger*, 1985]. There is more rapid transport from Europe and northern Asia to the Arctic [*Stohl*, 2006] than from more southern regions [*Hole et al.*, 2009] or North America. Measurements of trace metals from combustion (Mn, V) have been used to confirm the contributions of European sources to aerosol in the Arctic [*Rahn*, 1981]. Subsequent studies of the springtime Arctic haze have also linked contributions of sulfate aerosol to these metal tracers [*Quinn et al.*, 2009; *Rahn and McCaffrey*, 1980].

[3] Emissions from fuel-burning activities, including industry, electricity production, and domestic heating, have

[1]Scripps Institution of Oceanography, University of California, San Diego, La Jolla, California, USA.
[2]Department of Civil and Environmental Engineering, Massachusetts Institute of Technology, Cambridge, Massachusetts, USA.
[3]Aerodyne Research, Inc., Billerica, Massachusetts, USA.
[4]Pacific Marine Environmental Laboratory, NOAA, Seattle, Washington, USA.

Copyright 2011 by the American Geophysical Union.
0148-0227/11/2010JD015178

been identified as contributors to Arctic haze by chemical analyses of Arctic aerosol particles [*Ottar et al.*, 1986; *Rahn and McCaffrey*, 1979; *Rahn et al.*, 1977, 1989]. Chemical tracers for these types of anthropogenic emissions, such as sulfate, black carbon, Pb, Cd, Cu, and Zn, were found in Greenland snow [*Candelone et al.*, 1996; *Davidson et al.*, 1993; *Masclet et al.*, 2000], suggesting similar types of emission sources for these species and the constituents of Arctic haze. During the winter and early spring, fossil fuel combustion is the main source of sulfate to the Arctic since there is minimal biological activity [*Ferek et al.*, 1995]. Anthropogenic emissions from conurbations, such as Murmansk on the Kola peninsula, industrial emissions from the northern part of Russia, oil industry, and shipping all contribute to haze particles [*Hole et al.*, 2006a]. The Kola peninsula, in addition to other parts of northern Russia, has many Ni, Cu, and other non-ferrous metal producing industries, which also contribute to anthropogenic emissions [*Hole et al.*, 2006b; *Weiler et al.*, 2005].

[4] Recent evidence has shown that organic compounds comprise more than 30% of the submicron PM (PM_1) in Arctic Haze [*Shaw et al.*, 2010]. Aerosol haze particles are thought to be chemically aged, very efficient at scattering solar radiation, and possibly weakly absorbing of solar radiation [*Law and Stohl*, 2007]. Identifying the sources of the haze and determining its chemical composition is necessary to define and mitigate its climate impact on both the shortwave and longwave radiation balance in the Arctic [*Quinn et al.*, 2007]. Here, we use springtime measurements from the International Chemistry Experiment in the Arctic Lower Troposphere (ICEALOT) and from Barrow, Alaska, to characterize and contrast the composition and identify the sources of organic components that contribute to haze from the Atlantic and Pacific sides of the Arctic.

2. Methods

[5] As part of the 2008–2009 International Polar Year, submicron particles were measured aboard the R/V *Knorr* during ICEALOT (19 March 2008 to 24 April 2008) over the North Atlantic and Arctic Oceans and the Greenland, Norwegian, and Barents Seas (20°–30°W and 41°–81°N). Submicron particles were collected from an isokinetic sampling inlet 18 m above sea level that extended 5 m above the aerosol measurement container. The inlet was heated to dry the aerosol to a relative humidity (RH) of 25% or less, during sampling. Sector control for the flow was used to prevent sampling emissions directly from R/V *Knorr*. From 1 March 2008 to 1 March 2010, similar measurements were made at the National Oceanic and Atmospheric Administration Earth System Research Laboratory (NOAA ESRL) observatory at Barrow, Alaska, with an analogous collection method described by *Shaw et al.* [2010] for the 2008 samples. The Barrow sampling site is at a coastal location (156.6°W, 71.5°N) in the northern Pacific side of the Arctic. Sector control is used at Barrow to avoid emissions from the local town. This stops the sample collection when the wind direction is between 0 and 130 degrees, which reduced the sampling time by 35% for the 221 collected filters in this study.

2.1. Filter-Based Particle Collection

[6] During ICEALOT, submicron particles were collected on 37 mm Teflon filters for 12 and 24 h periods using the previously described isokinetic inlet. At Barrow, two years of near-continuous submicron particle measurements were collected using an automated rotating filter holder that exposed 47 mm Teflon filters to ambient air drawn into the warmed inlet at 30 L min^{-1} [*Quinn et al.*, 2002; *Shaw et al.*, 2010]. Filters at Barrow were exposed for different durations depending on season to accommodate changes in overall mass loadings: spring and winter filters were exposed for 24 h and summer filters for 96 h. After collection, the filters from both Barrow and the ICEALOT cruise were frozen, to prevent losses due to desorption or reaction, and transported back to San Diego for analysis by Fourier transform infrared (FTIR) spectroscopy. The FTIR spectra were analyzed using an automated algorithm that includes baselining, peak-fitting, and integrating at specific peak locations to quantify organic functional group mass associated with major carbon bond types based on the method outlined by *Maria et al.* [2002] and revised by *Russell et al.* [2009a]. Filters with detectable absorption at 876 cm^{-1} were rinsed with 2 mL of hexane, which removes the organosulfate containing compound without removing bisulfate or carbonate that also absorb in this region [*Blando et al.*, 1998; *Maria et al.*, 2003]. After the rinse, there was no absorbance remaining at 876 cm^{-1}, indicating efficient removal of organosulfate. Concentrations were calculated by dividing the mass of each functional group measured for each filter by the total volume of air sampled through the corresponding filters. Functional groups that were quantified include: hydroxyl (including alcohol, C-OH), alkane (C-CH), amine ($C\text{-}NH_2$), carbonyl (C=O), carboxylic acid (COOH), and organosulfate ($COSO_3$). Aromatic, alkene (C=CH), and organonitrate functional groups were below the detection limit for all filters discussed here.

[7] Prior to rinsing with hexane, X-ray Fluorescence (XRF; Chester LabNet, Tigard, Oregon) was performed on the FTIR analyzed filters to quantify the elemental mass concentrations of elements Na and heavier [*Maria et al.*, 2003]. For ICEALOT, S, K, Br, Ca, and Zn were measured above detection limit for 75% of the samples, Fe, Na, and Cl were above detection limit for 50% to 70%, and V and Si were above detection limit for between 35% and 40% of the samples. The remaining measured elements were above the detection limit for less that 15% of the samples and are not used in this analysis. Of the 221 filters collected from Barrow, a subset of 47 was analyzed by XRF for which Na, Cl, Fe, S, Br, K and Zn were consistently above detection limits [*Shaw et al.*, 2010]. The concentration of inorganic oxidized material (IOM – dust and fly ash) was calculated from the mass concentrations of Al, Si, Ca, Fe, and Ti assuming that each element was present in the aerosol in its most common oxide form [*Bates et al.*, 2008]. Because Al was below detection limit for all but one of the samples where V was above detection limit, the measured V was identified as non-crustal.

[8] Submicron particles (RH < 25%) were also collected with a Berner-type cascade impactor on Millipore Fluoropore filters downstream of a jet plate with a 50% aerodynamic cutoff diameter of 1 μm on the R/V *Knorr*. 1 mL of

spectral grade methanol was added to the filters followed by 5 mL of distilled, deionized water. The substrates were extracted by sonicating for 30 min. They were then analyzed by ion chromatography (IC) to quantify inorganic ions including sodium (Na^+), chloride (Cl^-), sulfate, nitrate, and ammonium [*Quinn et al.*, 1998]. Non-sea salt SO_4^{2-} concentrations were calculated from Na^+ concentrations and the ratio of SO_4^{2-} to Na^+ in seawater [*Quinn et al.*, 2000]. Sea salt concentrations were calculated from the measured concentrations of Na^+ and Cl^-, in order to take into account Cl^- depletion in the atmosphere [*Bates et al.*, 2008].

2.2. Aerosol Mass Spectrometry

[9] A quadrupole aerosol mass spectrometer (Q-AMS) was used to measure submicron particle composition averaged over 5-min intervals aboard the R/V *Knorr*. Non-refractory ions (chemical components that vaporize at 600°C) including sulfate (SO_4^{2-}), nitrate (NO_3^-), and ammonium (NH_4^+), were measured by Q-AMS, in addition to OM [*Allan et al.*, 2003; *Jayne et al.*, 2000]. A collection efficiency of 1 was used for all species described here based on the high acidity (low molar ratio of ammonium to sulfate) of measured particles and high relative humidity during measurements [*Matthew et al.*, 2008; *Quinn et al.*, 2006]. Comparisons of sulfate and ammonium concentrations measured by the Q-AMS and separately by IC of filter extracts were used to confirm the collection efficiency [*Hawkins et al.*, 2010; *Russell et al.*, 2010]. Sulfate measured by the Q-AMS was higher than that measured by IC (slope = 1.42, r = 0.82) suggesting sufficient collection by the Q-AMS. Ammonium measured by both instruments compared well (slope = 0.99, r = 0.75) further supporting a collection efficiency of 1. The total submicron OM (OM_1) measured by FTIR exceeds the OM_1 measured by the Q-AMS (slope = 0.91, r = 0.57) but is within the 20% uncertainty reported for either technique and is consistent with a reduced collection efficiency of organic mass on sea salt or other non-refractory particles [*Russell et al.*, 2010, 2009b].

[10] Submicron particle composition was also measured aboard the R/V *Knorr* using a high resolution time of flight aerosol mass spectrometer (HR-ToF-AMS, Aerodyne Research Inc., Billerica, MA) [*Canagaratna et al.*, 2007; *DeCarlo et al.*, 2006]. Measurements were made every minute alternating automatically between V and W mode, with and without a thermal denuder, and in combination with particle time of flight (PToF) mode. The HR-ToF-AMS data were analyzed using SQUIRREL and PIKA software (described at http://tinyurl.com/tofams-analysis) to determine the concentrations of mass fragments and common aerosol species [*Canagaratna et al.*, 2007; *DeCarlo et al.*, 2006]. The speciated HR-ToF-AMS mass concentrations correlated well with those obtained from the Q-AMS. An unknown problem caused the absolute concentrations determined by the HR-ToF-AMS to be unusually and systematically low throughout this campaign, so only the Q-AMS was used for quantitative mass concentrations of the major aerosol components. The high resolution mass spectra obtained from the HR-ToF-AMS were used to investigate the normalized oxygen to carbon (O/C) ratios of the observed organic aerosol. The organic aerosol was further characterized by positive matrix factorization (PMF) of HR-ToF-AMS organic mass spectra.

2.3. Potential Source Contribution Function

[11] A potential source contribution function (PSCF) was used to determine the regions that have higher probabilities of being sources for the input of aerosol mass [*Pekney et al.*, 2006]. This algorithm uses the calculated 5-day isentropic Hybrid Single Particle Lagrangian Integrated Trajectory (HYSPLIT) model to generate air mass back trajectories [*Draxler and Rolph*, 2003] with gridded frequencies of co-occurrence with high concentration samples. Back trajectories were calculated arriving at 500 m above the sampling platform every hour for ICEALOT and every 4 h for Barrow. PSCF analysis was calculated individually on the time series of concentrations and mass fractions of organic functional groups, total OM_1, PMF derived factors, and Q-AMS mass fragments.

3. Results

[12] Five aerosol source regions were identified along the ICEALOT cruise track based on HYSPLIT 5-day isentropic back trajectories [*Draxler and Rolph*, 2003]. The five regions, including three continental (Long Island, North American, and European) and two marine (North Atlantic and Arctic), are shown along the ship track in Figure 1. Particles from the marine source regions had carbohydrate-like OM_1 signatures mixed with sea salt and are described by *Russell et al.* [2010]. The continental regions differ from the marine regions in that they have higher OM_1, PM_1, and combustion tracer concentrations in addition to higher radon concentrations (European source region: 540 mBq m^{-3}) relative to the marine source regions (190 mBq m^{-3} for the Arctic and 340 mBq m^{-3} from the North Atlantic).

3.1. Particle Mass

[13] Average non-sea salt PM_1 concentrations from European, Long Island, and North American source regions were 2.75 ± 0.80, 3.40 ± 1.10, and 2.26 ± 0.76 μg m^{-3}, respectively. The European and Arctic regions have similar relative particle compositions (Figure 1). Overall during ICEALOT, non-sea salt sulfate was the dominant anthropogenic aerosol component and had the highest measured concentration levels with an overall mean of 1.06 ± 0.70 μg m^{-3}, which was 53% of the total PM_1 (Figure 2). The highest fractions of sulfate were measured from the European and Arctic source regions (58 and 64% of PM_1, respectively). Nitrate and ammonium levels were relatively low, accounting for less than 2% and 8% of the overall PM_1, respectively. At Barrow, the submicron particle composition had a larger fraction of OM_1 (35%; see Figure 1) and a comparable fraction of sea salt (13%) and IOM (8%).

[14] During ICEALOT, the ratio of non-sea salt sulfate to non-crustal V was 2.15 ± 1.39, overall. Previously reported values at Barrow, 3 [*Rahn and McCaffrey*, 1980] and 2.9–4.2 [*Quinn et al.*, 2009], are within the standard deviation of this average suggesting that similar source regions were being measured, specifically European. *Rahn and McCaffrey* [1980] state that the ratio measured at Barrow in 1976 and 1977 is an order of magnitude greater than ratios measured at midlatitudes. This suggests that the aerosol measured during ICEALOT also has contributions of secondary aerosol, like that measured previously at Barrow. The higher ratio (2.44) measured from the European source region suggests

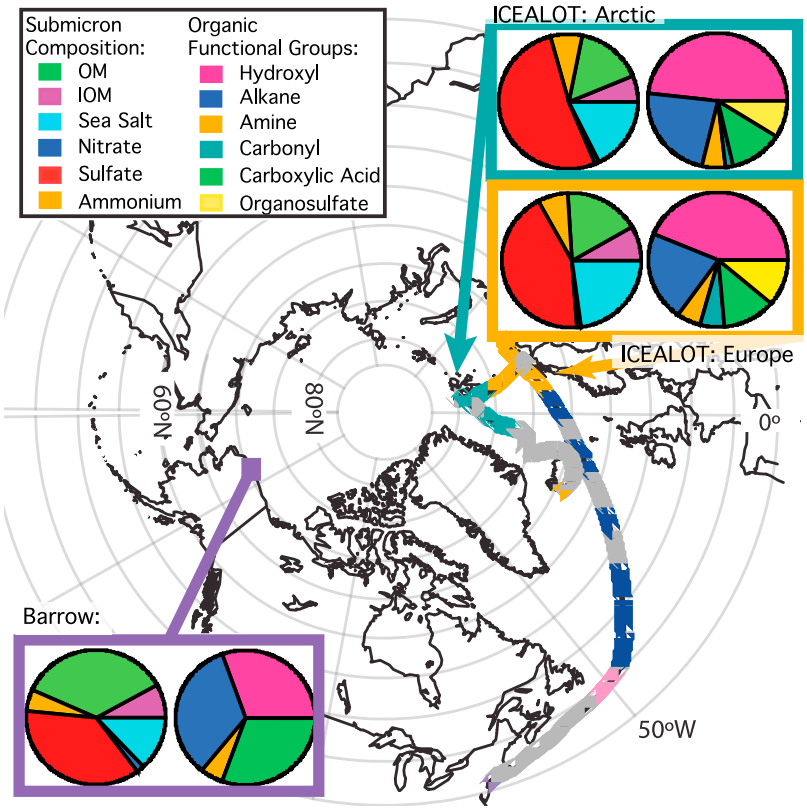

Figure 1. Track of the R/V *Knorr* during the ICEALOT cruise colored by regions of air mass origin including Long Island (purple), North America (pink), North Atlantic (dark blue), Europe (bronze), and Arctic (teal). The pies represent the submicron particle composition (left) and organic functional group composition (right) for the European and Arctic source regions during ICEALOT and Barrow (dark purple). The submicron particle composition excludes the elemental carbon (estimated on average less than 3% during ICEALOT and at Barrow).

that resulting aerosol from the European source region are more secondary and oxidized during transport.

3.2. Organic Mass

[15] Total OM_1 measured by FTIR was calculated by summing the concentrations of the functional groups on each filter. The average OM_1 concentration for ICEALOT (Figure 2) was 0.61 ± 0.36 μg m^{-3}. The highest concentrations (average: 0.89 ± 0.27 μg m^{-3}) were observed when sampling was from the European source region. For two years at Barrow, the average springtime OM_1 was 0.41 ± 0.36 μg m^{-3}. The organic functional group composition measured at Barrow had a larger fraction of alkane (34%) and carboxylic acid (30%) groups than the Arctic (23%, 13%) and European (21%, 12%) source regions measured during ICEALOT. In addition, organosulfate and non-acid carbonyl functional groups were measured in the Arctic and European source regions (on average 10% and 4%, respectively) and not observed at Barrow.

3.3. Ratio of Oxygen to Carbon

[16] The oxygenated fraction of organic aerosol has been used as an indicator of atmospheric processing and photochemical age [*Maria et al.*, 2004; *Zhang et al.*, 2005a]. The O/C ratio is sometimes an indicator of acid groups, which are a result of photochemical aging in the atmosphere. However, some oxygenated groups such as hydroxyl may also increase O/C, although they can originate from primary sources such as ocean-derived marine aerosol [*Russell et al.*, 2010].

[17] For ICEALOT, the O/C ratio was calculated by two methods. Oxygen-containing functional groups (hydroxyl, carboxylic acid, carbonyl, and organosulfate) from FTIR measurements were summed to give the contribution of oxygen atoms to the FTIR O/C ratio and normalized by the total number of carbon atoms from each measured functional group [*Hawkins et al.*, 2010; *Russell et al.*, 2009a]. Because hydroxyl was a large fraction of the OM_1 measured by FTIR, it had the largest contribution to the total O/C ratio, contributing on average 70% (0.66) of the total O/C. The O/C ratio calculated from the functional groups measured with FTIR spectroscopy was high (0.94) during ICEALOT indicating a highly oxygenated aerosol [*Russell et al.*, 2010]. The O/C from the European source region was 1.0, while the O/C in the Arctic source region was slightly lower (0.87) but still highly oxygenated.

[18] The HR-ToF-AMS O/C ratio was calculated from the individual abundances of O and C for each mass fragment using the Analytical Procedure for Elemental Separation (APES) included in the PIKA analysis software (described at http://tinyurl.com/tofams-analysis) [*Aiken et al.*, 2007, 2008]. In ambient environments, observed O/C values for oxidized secondary organic aerosol species range

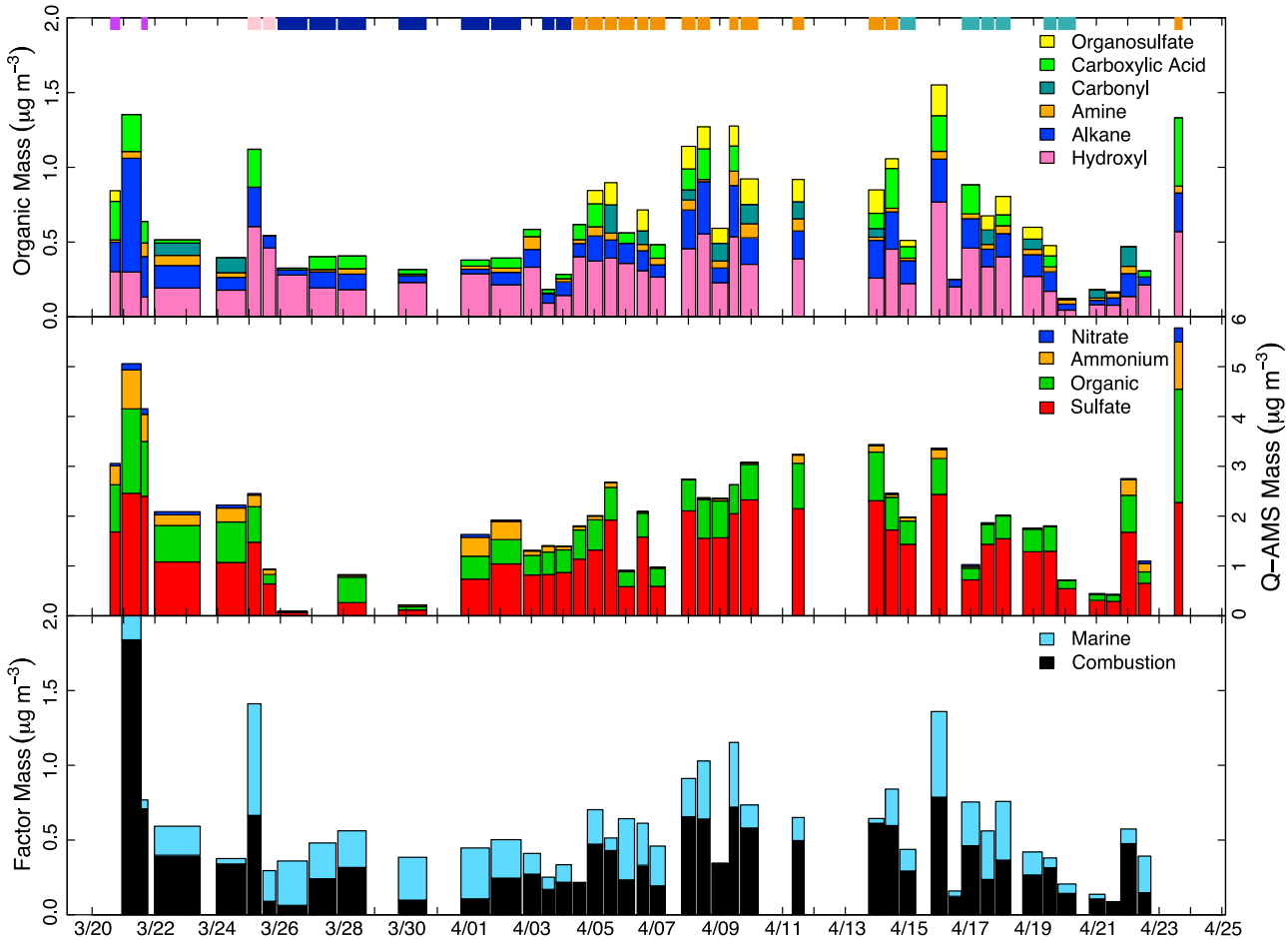

Figure 2. Time series and average composition of aerosol mass. Horizontal color bar: regions of air mass origin colored according to the ship track in Figure 1. Top panel: Functional group concentrations contributing to the total OM_1 measured by FTIR. Middle panel: Mass fragment contribution to total PM_1 measured by Q-AMS. Bottom panel: Factors contributing to organic mass derived from PMF on FTIR spectra.

from ~0.2 to ~0.9 [*Jimenez et al.*, 2009]. Primary urban vehicle emissions have very low AMS O/C ratios from 0.06–0.1 [*Aiken et al.*, 2008], and an O/C ratio greater than 0.40 is considered highly oxygenated [*DeCarlo et al.*, 2008]. The calculated O/C ratio for ICEALOT correlates well (r = 0.91) with the ratio of particulate CO_2 (at nominal *m/z* 44) to total OM_1 consistent with the relationship proposed by *Aiken et al.* [2008]. The ICEALOT campaign averaged HR-ToF-AMS based O/C ratio is 0.41. Aerosol measured from the European source region has an O/C of 0.44, while the Arctic source region aerosol has a larger O/C (0.60). Taken together, these results indicate that the ICEALOT aerosol was highly oxidized. The increase in O/C in the Arctic region is likely indicative of continued processing and aging of aerosols as they are transported from sources to the Arctic.

[19] In general, the HR-ToF-AMS O/C values are systematically lower than those measured by the FTIR. The mild correlation (r = 0.68) of the percent difference in the FTIR and HR-ToF-AMS O/C with the hydroxyl fraction of OM_1 suggests that this difference in the O/C of the two methods is likely due to the lower O/C observed for hydroxyl groups by the HR-ToF-AMS [*Aiken et al.*, 2007; *Hawkins et al.*, 2010]. The HR-ToF-AMS O/C correlates weakly with O/C calculated from only the FTIR carboxylic acid groups (r = 0.45 in the European source region, but r = 0.27 overall), which is consistent with the HR-ToF-AMS O/C correlation with the ratio of particulate CO_2 (at nominal *m/z* 44) to total OM_1, much of which is often attributed to acid mass fragments.

3.4. FTIR PMF

[20] Positive matrix factorization (PMF) was calculated for the FTIR spectra [*Paatero*, 1997; *Paatero and Tapper*, 1994] from the ICEALOT cruise and (separately) from the two-year Barrow data. A four-factor solution, which was recombined into two factors that were less correlated to each other in time, was found to best recreate the original ICEALOT time series (Figure 2), as previously discussed by *Russell et al.* [2010] (in the supporting information of that article). The two factors were determined to be a mixed combustion factor and a marine-derived factor (the latter of which is discussed in detail by *Russell et al.* [2010]). The mixed combustion factor was determined from correlations ($0.5 < r < 1$) with typical combustion tracers (S, Zn, K, Br) [*Qureshi et al.*, 2006; *Russell et al.*, 2009a; *Sharma and Maloo*, 2005] and large fractions of alkane and carboxylic

acid functional groups consistent with combustion factors, containing both primary and secondary aerosol, from previous studies [*Hawkins et al.*, 2010; *Russell et al.*, 2011, 2009a]; see also section 4.1. The time series reconstructed from the factors of OM_1 correlates well with the original FTIR OM_1 time series (r = 0.86). The correlation improves when the organosulfate functional group, which is not included in the wavelength range used for PMF, is removed from the FTIR OM_1 correlation (r = 0.89). The slope of the line (Factor OM_1 = 1.01*FTIR OM_1) shows that the factors provide a good representation of the OM_1 and its variations.

[21] For the Barrow time series, PMF was performed on the 221 spectra resulting in a two-factor solution with FPEAK = 0. The FPEAK = 0 rotation of the PMF solution was selected since there was little sensitivity to rotations with higher or lower FPEAK values. Furthermore, the first half of the time series (from 2008) had measurements of inorganic ions by IC and trace elements by XRF on the same filters that correlated strongly with signatures for each factor. The spectra of the factors from the updated PMF analysis for the full 221 filters at Barrow are indistinguishable from those obtained from the original 118 spectra from 2008 to 2009, so we applied the same source-based definitions. The first factor was determined to be a mixed combustion factor because it exhibits strong spectral signatures in the alkane and carboxylic acid regions of the IR spectrum and correlates with combustion and industrial tracers (V, K, Fe, Zn, Br, etc.). The other factor was defined as an ocean derived factor because it exhibits strong spectral signatures of marine hydroxyl groups similar to those of ICEALOT described by *Russell et al.* [2010], correlated strongly with Na^+ and Cl^- associated with sea salt, and corresponded to air masses that originated from open ocean in summer [*Shaw et al.*, 2010].

3.5. AMS PMF

[22] PMF was used for the organic portion of the HR-ToF-AMS mass spectrum calculated at unit mass resolution [*Allan et al.*, 2004b; *Ulbrich et al.*, 2009]. All analysis for HR-ToF-AMS PMF was done using PMF2 in robust mode [*Paatero*, 1997; *Paatero and Tapper*, 1994]. The PMF Evaluation Tool (PET) developed in Igor Pro (Wavemetrics, Inc., Portland, Oregon), described by *Ulbrich et al.* [2009], was used to evaluate the PMF output for HR-ToF-AMS spectra, with additional details provided in Appendix A.

[23] The three factors of the solution that best reconstructs the OM time series are: (1) an oxygenated organic aerosol (OOA) factor, with intense *m*/*z* 44 signal; (2) a hydrocarbon-like organic aerosol (HOA) factor, characterized by hydrocarbon ion fragments (*m*/*z* 41, 43, 55, 57, 67, 69, 71, etc.); and (3) a third factor (F3) with unique ion fragments (*m*/*z* 50–55, 65, 67, 77, 79, 91). The time series and spectra of the factors are shown in Figures 3a and 3b.

[24] The OOA factor contributes 33% to the ICEALOT project average OM_1 and 31% in the European source region. The OOA factor spectrum correlates strongly with the reference spectra of oxalic, glyoxcylic, and fulvic acids (r = 0.94, r = 0.93, r = 0.84, respectively) [*Alfarra*, 2004; *Takegawa et al.*, 2007] from the AMS spectral database (I. M. Ulbrich et al., http://cires.colorado.edu/jimenez-group/AMSsd/) described by *Ulbrich et al.* [2009], providing an indication that this highly oxygenated factor is representative of acid-containing organic aerosol. The OOA factor correlates mildly in time with the FTIR measured carboxylic acid functional group (r = 0.49 overall, r = 0.71 in the European source region) consistent with the interpretation of the OOA factor as an acid-containing, secondary, aged, organic component. The time series of the OOA factor also correlates (r = 0.67) with sulfate, consistent with other measurements in eastern Europe [*Lanz et al.*, 2007].

[25] The HOA factor is present mainly at the start of the cruise in the Long Island and North American source regions. HOA contributes 28% to the total OM_1 and 29% and 41% in the Long Island and North American source regions, respectively. The HOA factor spectrum correlates strongly with HOA spectra measured in other campaigns (r = 0.99 and r = 0.98) [*Lanz et al.*, 2009; *Zhang et al.*, 2005b] and also diesel bus exhaust (r = 0.98) [*Canagaratna et al.*, 2004; *Ulbrich et al.*, 2009]. In addition, the HOA factor correlates (r = 0.68) with NO_X (measured on board the R/V *Knorr* using the method described by *Lerner et al.* [2009]), consistent with less processed emissions [*Lanz et al.*, 2007]. HOA is lower in the European source region (20%) where there is a longer distance between emissions and sampling, suggesting that the emissions measured in the European source region had been processed more or longer in the atmosphere.

[26] The OOA factor and the FTIR combustion factor show a correlation of r = 0.42 overall and r = 0.74 for the European source region, which is consistent with the large contribution of carboxylic acid functional groups to the FTIR combustion factor. The HOA factor has a moderate correlation with the FTIR combustion factor (r = 0.51), but the correlation to the FTIR combustion factor is higher for the sum of OOA and HOA (r = 0.67 overall and r = 0.64 for the European source region; see Figure 3c). This suggests that the FTIR combustion factor includes both hydrogenated and oxygenated carbon mass fragments, likely including a range of recent and more processed components of combustion emissions. In the European source region, the stronger correlation of the FTIR combustion factor with OOA than with OOA + HOA suggests that the FTIR combustion factor OM_1 from that region is more processed.

4. Discussion

4.1. Combustion Sources of Organic Mass in Arctic Haze

[27] Emissions from combustion sources provide a large fraction of the aerosol mass in the Arctic that makes up the springtime Arctic haze. Recent measurements at Barrow and during ICEALOT show that the combustion sources typically contribute more than half of OM_1 and over a quarter of PM_1, based on FTIR, AMS, and IC analyses. A comparison of aerosol measured during the spring in these two regions of the Arctic provides insight into the differences in emission sources and regions contributing to the springtime Arctic haze. The large fraction of oxygenated functional groups measured in the Arctic indicates a high O/C fraction close to 1 (discussed in section 3.3), which is consistent with an aged combustion source and indicates one oxygen for every carbon in an organic particle [*Jimenez et al.*, 2009; *Russell et al.*, 2010, 2009a]. Emissions from coal combustion in northeastern Europe contribute to the OM_1 measured

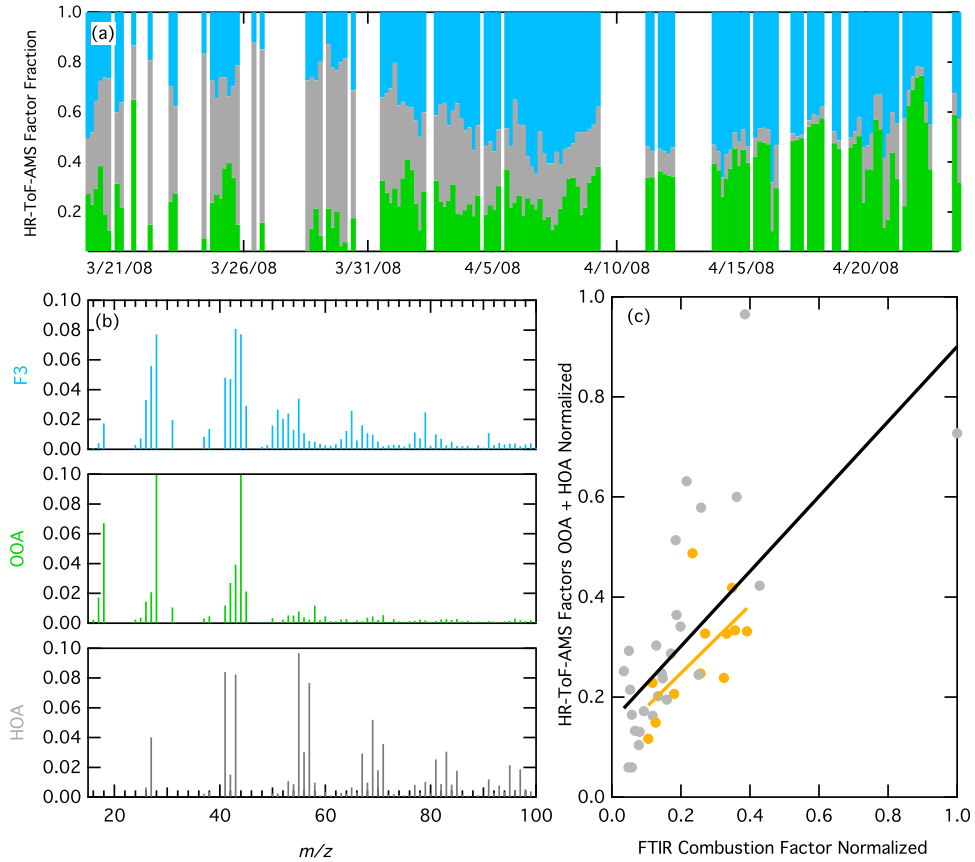

Figure 3. (a) Time series of HR-ToF-AMS factor fractions of total OM including HOA (dark gray), OOA (green), and F3 (light blue). (b) The mass spectra of the three distinct factors: HOA, OOA, and F3. (c) Comparison between the HR-ToF-AMS factors OOA + HOA (normalized by the maximum value) and the FTIR combustion factor (normalized by the maximum value), r = 0.64 overall (black) and r = 0.64 in the European source region (orange).

in the northern Atlantic region of the Arctic, while biomass burning, shipping, and industrial emissions contribute to the OM_1 measured in the northern Pacific region of the Arctic.

4.1.1. Combustion Factor Contribution to OM_1

[28] PMF of both ICEALOT and Barrow FTIR spectra provide evidence for combustion factors that constitute more than 60% of the OM_1 measured at both sites. The combustion factors show significant fractions of alkane, hydroxyl, and carboxylic acid functional groups. During ICEALOT, the combustion factor was 63% of the total OM_1 and contributed 0.36 ± 0.31 $\mu g\ m^{-3}$ to the total organic mass (Figure 2). When the aerosol originated from the European source region, the combustion factor was 68% of the total OM_1 and contributed 0.47 ± 0.18 $\mu g\ m^{-3}$. Since OM_1 was approximately 33% of the overall PM_1 and 43% in the European air mass source region, this large contribution of combustion sources from Europe provided a substantial part of the Arctic haze aerosol concentrations in the Barents and Greenland Sea regions during the ICEALOT cruise.

[29] Measurements taken in Barrow, Alaska, span two years and three different seasons (spring, summer and winter). The Barrow spring season was defined to represent the high OM_1 concentrations that prevail in March through June [*Shaw et al.*, 2010] and includes the ICEALOT sampling period. The OM_1 measured during spring in both 2008 and 2009 at Barrow was higher (0.41 ± 0.36 $\mu g\ m^{-3}$) than the average OM_1 measured both years (0.32 ± 0.36 $\mu g\ m^{-3}$). Most (80% or 0.32 ± 0.22 $\mu g\ m^{-3}$) of the OM_1 measured in the spring was attributed to combustion sources based on correlations with trace metals in spring 2008 [*Shaw et al.*, 2010]. The OM_1 concentration and fraction of the combustion factor were significantly higher than the annual average combustion OM_1 (0.19 ± 0.21 $\mu g\ m^{-3}$), indicating that combustion sources also had a substantial impact at Barrow on the OM_1 fraction of springtime Arctic haze.

4.1.2. Combustion Factor Composition

[30] The spectra of the combustion factors for aerosol measured in the northern Pacific and northern Atlantic regions of the Arctic are similar (Figure 4a). The differences between the two combustion factor spectra may result both from differences in their source emissions (i.e., between the mixture of combustion sources in Siberia and those in eastern Europe) and in their atmospheric oxidation processes. The ICEALOT combustion factor OM_1 includes large mass fractions of hydroxyl (36%), alkane (35%), and carboxylic acid (27%) functional groups, with a minor fraction (3%) of amine groups (Figure 4a). The large fraction of carboxylic acid functional groups suggests that particles aged from combustion emissions contribute to this factor [*Maria et al.*, 2004; *Zhang et al.*, 2005a]. The Barrow combustion factor

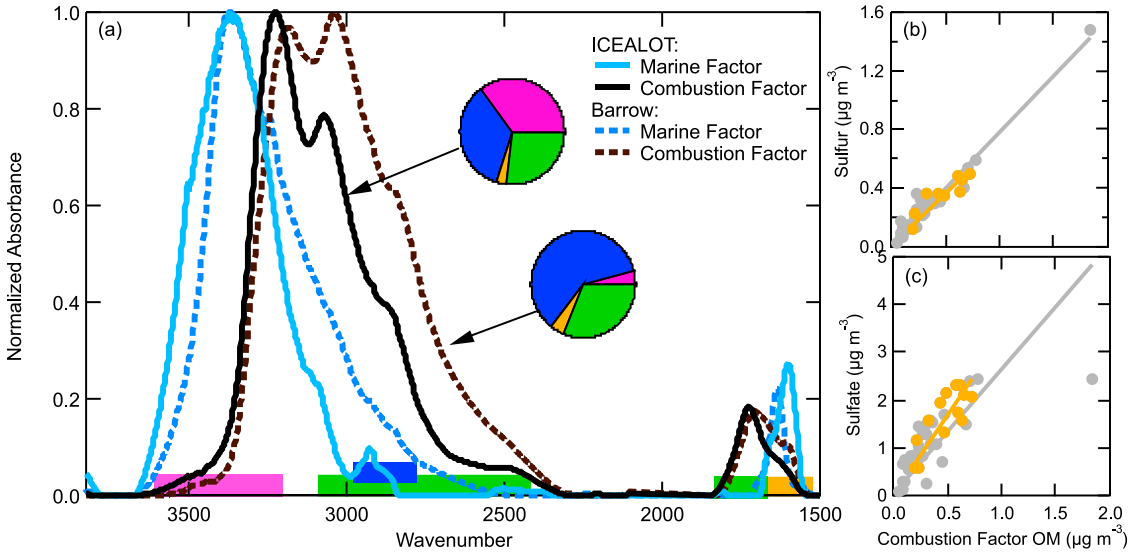

Figure 4. (a) Factor spectra from PMF of FTIR sample spectra for ICEALOT (solid) and Barrow (dashed). The pie charts show the average composition of the combustion factor, using the colors described in Figure 1, for both ICEALOT and Barrow. Comparisons of the ICEALOT combustion factor with (b) S (r = 0.97, r = 0.9) and (c) sulfate (r = 0.75, r = 0.8) for all air masses (gray) and the European source region (orange), respectively.

for the full 2-year study consists of alkane (60%) and carboxylic acid (31%) groups and smaller fractions of amine (5%) and hydroxyl (4%) groups (Figure 4a). The large fraction of alkane groups suggests that the combustion emissions contributing to this factor may have undergone less atmospheric processing than those measured during ICEALOT.

[31] The combustion factors retrieved from the organic FTIR spectra for both ICEALOT and Barrow have large contributions from both carboxylic acid and hydroxyl functional groups. These oxygenated groups are characteristic of the products expected from photochemical oxidation [*Huebert and Charlson*, 2000; *Lim and Ziemann*, 2005, 2009; *Putaud et al.*, 2000] indicating that the measured particles are due in part to secondary organic aerosol. The weakness of the correlations during ICEALOT to elemental tracers (Fe and V) indicates that the variability in the combustion factor OM may lag the primary combustion products, which is expected for secondary rather than primary OM.

4.1.3. Sources of Combustion in Northeastern Europe and Asia

[32] The combustion factor derived from measurements in the north Atlantic and adjacent regions of the Arctic Ocean during ICEALOT reflects aerosol influenced by emissions from northeastern Europe and Russia. Coal burning is one of the main sources of heating, and there are also numerous coal burning smelters in that area [*Hole et al.*, 2006a; *Tzimas et al.*, 2009; *Weiler et al.*, 2005]. The Kola Peninsula, northeast of Finland, has Cu and Ni producing industry which emits high levels of SO_2 and NO_2 [*Weiler et al.*, 2005]. In the Kola Peninsula, the conurbation of Murmansk is a highly populated metropolitan area and sea port, which contributes to the polluted air from that area [*Law and Stohl*, 2007]. The combustion factor concentration correlates strongly with S concentrations for both overall (r = 0.97) and the European source region (r = 0.90; see Figure 4b) indicating that coal burning is likely collocated or co-emitted with the organic combustion sources. This strong correlation of the combustion factor OM_1 with sulfur likely is a consequence of S being primarily sulfate, a typical secondary aerosol product of coal combustion emissions, which also correlates strongly with r = 0.75 overall (and r = 0.80 in the European source region; see Figure 4c) suggesting that the sources of the organic combustion factor and those of the sulfate are collocated. Correlations with Zn (total r = 0.74; European source region r = 0.57) are consistent with emissions from non-ferrous metal producing industries, such as copper smelting in northeastern Europe [*Polissar et al.*, 1998, 2001; *Shaw*, 1982]. The combustion factor weakly correlates with V (r = 0.24 overall, r = 0.44 in the European source region), suggesting that the combustion factor may also have some contributions from oil burning. The ratio of non-sea salt sulfate to non-crustal V mildly correlates (r = 0.55) in the European source region with the combustion factor fraction of OM. In addition to the correlations with the combustion and pollution tracers (Zn, Ca, Fe, S, and V), the concentrations of these metals were 5–65% higher in the European source region than the ICEALOT average.

[33] About 50% of Europe's electricity is produced from fossil fuel combustion [*Tzimas et al.*, 2009], and high alkane concentrations are found in petroleum combustion emissions from Europe [*Blake et al.*, 1994, 2003]. In eastern Europe, combustion of fuels such as coal and lignite lead to high levels of SO_x, NO_x, PM, and CO_2 emissions [*Ross et al.*, 2002]. The mixture of high SO_x emissions from coal and alkane emissions from petroleum could explain the correlation of the organic combustion factor and the sulfate observed during the European source region of the ICEALOT cruise, making emissions from northeastern Europe the main source of OM_1 in the Arctic haze on the northern Atlantic side.

[34] At Barrow, the combustion factor also correlates strongly to S but, in addition, is correlated to non-dust K,

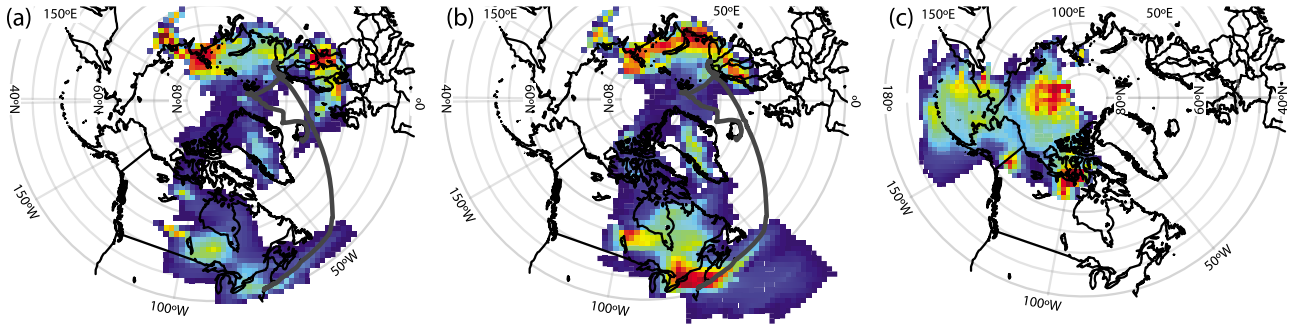

Figure 5. PSCF of (a) the total OM_1 measured during ICEALOT, (b) the ICEALOT combustion factor, and (c) the Barrow combustion factor. The higher potential source regions are indicated by red and the lower potential source regions are indicated with blue.

characteristic of a biomass burning source, where [non-dust K] = [K] − 0.62*[Al] [*Cachier et al.*, 1995; *Gilardoni et al.*, 2009]. Alaskan and Siberian wildfires were observed in spring 2008 and 2009 [*U.S. Department of Agriculture*, 2010; *Shaw et al.*, 2010; *Warneke et al.*, 2009], which provide evidence for the influence of biomass burning in the combustion factor. V, which is characteristic of processed emissions from oil burning, is mildly correlated with the combustion factor. V is a tracer for the combustion of heavy residual oil only used in the sub-Arctic since it is too viscous to use at cold temperature and is hence a tracer of the long range transport of emissions from oil combustion [*Isakson et al.*, 2001].

[35] To investigate the probability that these two different urban and industrial centers were the emission sources that were responsible for the observed high OM_1 from combustion factors, PSCF were calculated for Barrow and ICEALOT [*Pekney et al.*, 2006]. The region with high potential of being a source of the ICEALOT combustion factor is northeastern Europe, with the highest potential sources shown in Figure 5b as Scandinavia and the Kola Peninsula, as well as the northwestern edge of Russia. These areas of northeastern Europe have significant industrial activity, including non-ferrous metal producing plants that contribute to the organic emissions [*Blake et al.*, 2003; *Hole et al.*, 2006a; *Mira-Salama et al.*, 2008; *Weiler et al.*, 2005]. The PSCF of sulfate measured during ICEALOT shows a trend similar to the potential source of the organic combustion factor (see Figures 6a and 5b for comparison), supporting the suggestion that the organic and sulfate sources are collocated. In addition, PSCF for OM_1 measured during ICEALOT also shows potential sources in northeastern Europe (Figure 5a). PSCF of the Barrow combustion factor shows potential sources from northeastern Asia, shipping lanes in the Bering Strait, and along the Canadian-Alaskan border (Figure 5c), which are similar to the potential sources observed in 2008. The differences in the potential source regions shown in Figure 5 highlight the importance of northeastern Asian sources for Arctic haze at Barrow in contrast to the northeastern European sources of the Arctic haze during ICEALOT.

[36] In summary, the functional group composition indicates that the majority of the organic aerosol in Arctic haze is produced from combustion emissions, and back trajectories from both regions suggest that the combustion sources are in northeastern Europe and Asia. The two different sources of measured Arctic aerosol are demonstrated in the differences between the composition of their combustion factors and the potential source regions determined from PSCF.

4.2. Organosulfate Formation From Combustion Emissions

[37] One interesting chemical consequence of the co-emissions of sulfate from coal burning and volatile organic compound (VOC) emissions in northeastern Europe is the production of organosulfate functional groups. In air masses sampled from both the European and Arctic source regions of the ICEALOT campaign, organosulfate groups contributed 9% and 11% of the organic mass, respectively, whereas no organosulfate groups were measured at Barrow. The organosulfate functional group fraction of PM_1 has a strong correlation (r = 0.84) with the sulfate fraction of PM_1 for the European region and a moderate correlation (r = 0.50) for the entire ICEALOT cruise (Figure 7b) and was only detected in samples with sulfate concentrations greater than 1.25 $\mu g\ m^{-3}$. This observed increase in organosulfate group fraction of PM_1 with increased sulfate fraction of PM_1 is consistent with organosulfate formation on sulfate particles, many of which are likely acidic in this region [*Surratt et al.*, 2007a]. The molar ratio of ammonium to sulfate was 1.13 for the whole project and 1.22 during the periods of filter sampling. The lower average molar ratio of ammonium to sulfate (0.96) of particles measured from the European and Arctic source regions and their implied higher acidity provides conditions consistent with the acid-catalyzed particle-phase formation of organosulfate in air masses from those source regions [*Iinuma et al.*, 2009, 2007; *Liggio et al.*, 2005; *Perri et al.*, 2010; *Surratt et al.*, 2007a, 2010, 2007b, 2008]. Organosulfate group fraction of PM_1 has a mild negative correlation (r = −0.50) with relative humidity for the European source region (Figure 7c). In addition, organosulfate group concentration is mildly negatively correlated (r = −0.64) with absolute humidity in the European source region. These relationships suggest that organosulfate formation decreases with higher aerosol water concentrations, which may be due in part to the decrease in aerosol acidity with an increase in relative humidity (r = 0.52 overall, r = 0.51 for the European source region), consistent with the findings of a previous study in the southeastern Pacific [*Hawkins et al.*, 2010; *Liggio et al.*, 2005]. In summary, four conditions coincide with organosulfate group formation in the European and Arctic source regions, relative to the ICEALOT measurement

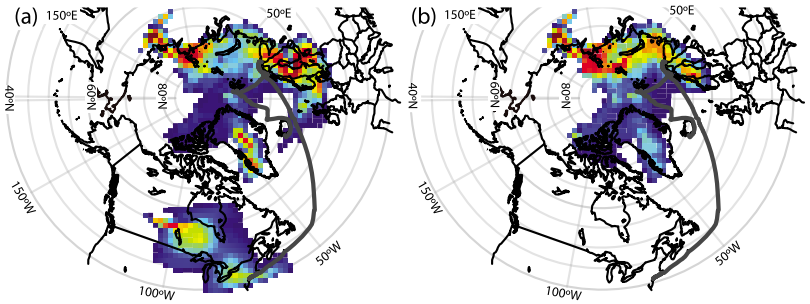

Figure 6. PSCF of (a) sulfate and (b) organosulfate functional group concentrations. The higher potential source regions are indicated by red and the lower potential source regions indicated with blue.

period: high organic mass (>0.75 μg m^{-3}), high sulfate (>1.25 μg m^{-3}), low ammonium to sulfate ratio (<1.0), and high overall relative humidity (>50%). These observations are consistent with sulfate particles providing acidic aqueous conditions that enhance organosulfate formation from organic precursors. The correlation of the sulfate and the organosulfate fractions of PM_1 also suggests both similar sources and similar processing times in the atmosphere (given the time resolution of the filter sampling, namely 12 h).

[38] The four conditions for organosulfate formation observed during ICEALOT did not all occur at Barrow, which could explain the lack of organosulfate formation there. During the spring seasons, the average sulfate concentration measured at Barrow was 0.64 μg m^{-3}, which is less than observed during ICEALOT but consistent with the range reported by *Quinn et al.* [2002] for the spring seasons of 1998–2000. On the other hand, the average molar ratio of ammonium to sulfate (0.75) was consistent with the acidic ratio measured during ICEALOT. Average OM_1 concentration (0.70 μg m^{-3}) measured during the spring season is slightly less than was observed for periods with organosulfate functional groups during ICEALOT. The process of acid-catalyzed particle haze formation of organosulfate likely does not occur during the spring seasons at Barrow.

[39] The sum of S (μmol m^{-3}) from inorganic sulfate measured by IC and organosulfate groups measured by FTIR correlates well (r = 0.92) with the total S measured by XRF (Figure 7a). Without the organosulfate group component, there is still a strong correlation (r = 0.92) to elemental (XRF) S, but the slope of the line (0.94) suggests that there is a missing source of S. When organosulfate is added to the IC measured sulfate, the total S is better represented, with a slope of 1.02. This suggests that the majority (94%) of the S concentration measured during ICEALOT is inorganic sulfate, with the remaining 6%, on average, coming from organic sulfate. The S from Q-AMS measurements of sulfate also correlates well (r = 0.91) with XRF measurements of S, consistent with the expectation that the Q-AMS detects both organic and inorganic sulfate [*Allan et al.*, 2004a; *Farmer et al.*, 2010].

[40] Using PSCF, the highest potential source contributions of the ICEALOT sulfate concentrations were found in northeastern Europe, similar to the locations of potential sources for the combustion factor, as is evident by comparing Figures 5b and 6a. In addition, the potential source of organosulfate groups is collocated with sulfate, as shown in Figure 6b.

[41] Other studies have shown organosulfate formation from biogenic precursors [*Gómez-González et al.*, 2008;

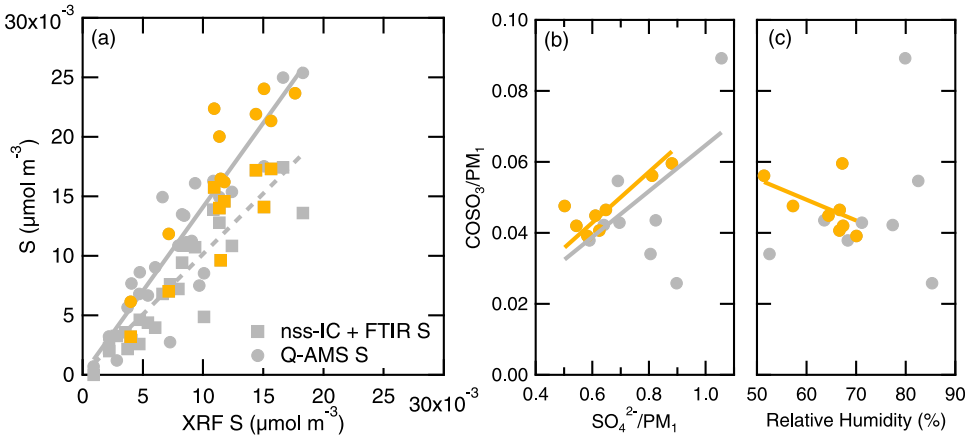

Figure 7. (a) Comparison of S measured by XRF with IC + FTIR derived S (slope = 1.02, r = 0.92) and Q-AMS derived S (y = 1.41, r = 0.91) for the total project (gray) and the European source region (orange). (b) Correlation of organosulfate group fraction of PM_1 with sulfate fraction of PM_1 (r = 0.84 for the European source region). (c) Negative correlation of organosulfate group fraction of PM_1 and relative humidity (r = −0.50 for the European source region).

Iinuma et al., 2009; *Surratt et al.*, 2007a, 2010, 2008]. Because there were no large sources of terrestrial biogenic emissions measured during ICEALOT, biogenic precursors during ICEALOT were not identified as a likely source of organosulfate functional groups. While the emissions from the European source region measured during ICEALOT have been attributed to fossil fuel burning, due to the absence of biogenic volatile organic compounds (BVOCs) in the air measured at the ship, it remains possible that co-located BVOCs did contribute to OM and to subsequent reactions with sulfate in particles to form organosulfate. *Claeys et al.* [2010] found evidence that organosulfate functional groups can occur with acidic particles produced from oxidation productions of dimethyl sulfide (DMS) and bacteria sources in a clean marine environment. The organosulfate measured during ICEALOT was unlikely to be the result of marine emissions since organosulfate functional groups were only observed when air masses were from European and Arctic source regions. Organosulfate group concentrations or fractions did not correlate with the marine factor, as would be expected for marine sources.

5. Conclusions

[42] Emissions from combustion sources greatly impact the concentrations of submicron aerosol particles in the Arctic and contribute to Arctic haze in both the Atlantic and Pacific sides of the Arctic region. Complementary measurement techniques show higher OM_1 in air masses sampled from the European source regions than from the marine source regions, both measured on the Atlantic side of the Arctic during ICEALOT. A large fraction (74%) of the OM_1 was attributed to eastern European combustion sources (industrial and other petroleum burning) based on PMF-derived factors from FTIR measurements. Measurements from Barrow, Alaska, on the Pacific side of the Arctic show the largest percent of OM_1 from mixed combustion sources (biomass burning and shipping) in the spring season. The organic functional group compositions indicate that mixed combustion sources account for more than 60% (>0.3 μg m^{-3}) of the total organic mass measured in air masses influenced from both the European and Arctic source regions during ICEALOT and the spring season at Barrow.

[43] Carboxylic acid and hydroxyl groups account for more than 35% of the combustion factor organic functional groups in the Atlantic and Pacific sides of the Arctic, reflecting the products of oxidation of emissions from fuel burning. The ICEALOT combustion factor, dominated by carboxylic acid, alkane, and hydroxyl functional groups, correlates well with sulfate suggesting that their sources are collocated. The large fraction of the carboxylic acid functional group is consistent with the secondary products expected from oxidation of VOCs. Q-AMS and HR-ToF-AMS measurements confirm the highly oxygenated nature of the OM_1 from combustion, with an OOA spectrum similar to that of oxygenated acid groups. Aerosol measured in the Pacific side of the Arctic at Barrow has a larger fraction of alkane suggesting that the aerosol is less aged. The differences in the combustion-derived spectra from the two regions result from the mixtures of sources in each region, although more specific contributions could not be resolved in these campaigns.

[44] On the Atlantic side of the Arctic, high levels of sulfate and OM_1 were typically associated with back trajectories that originated in northeastern Europe. The correlations between the combustion factor for ICEALOT and S and sulfate suggest emissions from the high coal burning regions of northeastern Europe. On the other hand, the correlations between the Barrow combustion factor and V and non-dust K are characteristic of emissions from northern Asia, Siberia, and, to a lesser extent, interior regions of Alaska and Canada.

[45] The high emissions of sulfate from coal-burning in northeastern Europe produce significant concentrations of the organosulfate functional groups that account for as much as 10% of OM_1 measured by FTIR over the Barents and Greenland seas during ICEALOT. There is some evidence suggesting that organosulfate formation occurs heterogeneously when compounds react in acidic (aqueous) sulfate particles. Organosulfate functional groups were measured in air masses from both the European and Arctic source regions, when high concentrations (1.25–2.40 μg m^{-3}) of sulfate were present but not at Barrow, which had lower sulfate concentrations (0.64 μg m^{-3}, average). The potential source region of organosulfate groups is collocated with the potential source region of sulfate during ICEALOT, where there are high S emissions from abundant sources of coal combustion. The high correlation between the organosulfate fraction of PM_1 and sulfate fraction of PM_1 and the low molar ratio of ammonium to sulfate (high acidity) suggests that organosulfate functional groups are formed on sulfate particles through acid-catalyzed aqueous reactions.

[46] Our findings suggest that pan-Arctic air quality is not uniform in composition but rather regionally dependent on different transport mechanisms and source regions. Since these unique aerosol contributions produce different chemical and microphysical consequences, climate models that are able to simulate direct and indirect aerosol effects must be able to treat the specific areas differently in order to make predictions of radiative forcing in the Arctic.

Appendix A: PMF of HR-ToF-AMS

[47] Unit mass resolution PMF analysis was performed on the HR-ToF-AMS data. The PET software and analysis methods outlined by *Ulbrich et al.* [2009] were used to perform the PMF analysis. The data and error matrices input into the PMF analysis were obtained with the SQUIRREL analysis program (described at http://tinyurl.com/tofams-analysis) [*Allan et al.*, 2003, 2004b]. The error matrices account for Poisson statistics in ion counting. A minimum error constraint was additionally placed on the error matrix according to *Ulbrich et al.* [2009]. Due to low signal to noise (S/N), ion fragments with masses above *m*/*z* 200 were removed from the analysis. The remaining ion fragments with $0.2 < S/N < 2$ were downweighted by a factor of 3 [*Ulbrich et al.*, 2009]. PMF analysis results were compared for solutions with 1 through 10 factors. The largest drop in Q/Qexpected occurred going from 1 to 2 factors, showing that at least two factors are needed to accurately represent the organic mass and explain the variance. The three factor solution, which had a minimum Q value and did not show any evidence of factor splitting, was chosen as the optimum solution for this analysis. The three factors together account

for 97% of the observed OM. The effect of rotation on the PMF solution was examined by changing the FPEAK parameter from −1 to 1 with 0.2 intervals. Solutions with $-0.22 < \text{FPEAK} < 0$ yielded component spectra and time series that did not contain unreasonable zeros. The chosen solution is supported by the strongest correlations with reference spectra posted at http://cires.colorado.edu/jimenez-group/AMSsd/ [*Ulbrich et al.*, 2009].

[48] **Acknowledgments.** This study was funded by the National Science Foundation (ATM-0744636; ARC-0714052) as part of the International Polar Year. We would like to thank John Ogren, Pat Sheridan, Anne Jefferson, and the staff of the NOAA ESRL Barrow station for guidance and assistance in the collection of the particle measurements discussed here. The authors would also like to acknowledge Brian Lerner at NOAA ERSL for the collection and interpretation of NO_X data during ICEALOT.

References

Aiken, A. C., P. F. DeCarlo, and J. L. Jimenez (2007), Elemental analysis of organic species with electron ionization high-resolution mass spectrometry, *Anal. Chem.*, *79*(21), 8350–8358, doi:10.1021/ac071150w.

Aiken, A. C., et al. (2008), O/C and OM/OC ratios of primary, secondary, and ambient organic aerosols with high-resolution time-of-flight aerosol mass spectrometry, *Environ. Sci. Technol.*, *42*(12), 4478–4485, doi:10.1021/es703009q.

Alfarra, M. R. (2004), Insights into atmospheric organic aerosols using an aerosol mass spectrometer, Ph.D. thesis, Inst. of Sci. and Technol., Univ. of Manchester, Manchester, U. K.

Allan, J. D., J. L. Jimenez, P. I. Williams, M. R. Alfarra, K. N. Bower, J. T. Jayne, H. Coe, and D. R. Worsnop (2003), Quantitative sampling using an Aerodyne aerosol mass spectrometer: 1. Techniques of data interpretation and error analysis, *J. Geophys. Res.*, *108*(D3), 4090, doi:10.1029/2002JD002358

Allan, J. D., et al. (2004a), Submicron aerosol composition at Trinidad Head, California, during ITCT 2K2: Its relationship with gas phase volatile organic carbon and assessment of instrument performance, *J. Geophys. Res.*, *109*, D23S24, doi:10.1029/2003JD004208.

Allan, J. D., et al. (2004b), A generalised method for the extraction of chemically resolved mass spectra from Aerodyne aerosol mass spectrometer data, *J. Aerosol Sci.*, *35*(7), 909–922, doi:10.1016/j.jaerosci.2004.02.007.

Bates, T. S., et al. (2008), Boundary layer aerosol chemistry during TexAQS/GoMACCS 2006: Insights into aerosol sources and transformation processes, *J. Geophys. Res.*, *113*, D00F01, doi:10.1029/2008JD010023.

Blake, D. R., T. W. Smith Jr., T.-Y. Chen, W. J. Whipple, and F. S. Rowland (1994), Effects of biomass burning on summertime nonmethane hydrocarbon concentrations in Canadian wetlands, *J. Geophys. Res.*, *99*(D1), 1699–1719, doi:10.1029/93JD02598.

Blake, N. J., D. R. Blake, B. C. Sive, A. S. Katzenstein, S. Meinardi, O. W. Wingenter, E. L. Atlas, F. Flocke, B. A. Ridley, and F. S. Rowland (2003), The seasonal evolution of NMHCs and light alkyl nitrates at middle to high northern latitudes during TOPSE, *J. Geophys. Res.*, *108*(D4), 8359, doi:10.1029/2001JD001467.

Blando, J. D., R. J. Porcja, T.-H. Li, D. Bowman, P. J. Lioy, and B. J. Turpin (1998), Secondary formation and the Smoky Mountain organic aerosol: An examination of aerosol polarity and functional group composition during SEAVS, *Environ. Sci. Technol.*, *32*(5), 604–613, doi:10.1021/es970405s.

Cachier, H., C. Liousse, P. Buat-Menard, and A. Gaudichet (1995), Particulate content of savanna fire emissions, *J. Atmos. Chem.*, *22*(1–2), 123–148, doi:10.1007/BF00708185.

Canagaratna, M. R., et al. (2004), Chase studies of particulate emissions from in-use New York City vehicles, *Aerosol Sci. Technol.*, *38*(6), 555–573, doi:10.1080/02786820490465504.

Canagaratna, M. R., et al. (2007), Chemical and microphysical characterization of ambient aerosols with the aerodyne aerosol mass spectrometer, *Mass Spectrom. Rev.*, *26*(2), 185–222, doi:10.1002/mas.20115.

Candelone, J.-P., J.-L. Jaffrezo, S. Hong, C. I. Davidson, and C. F. Boutron (1996), Seasonal variations in heavy metals concentrations in present day Greenland snow, *Sci. Total Environ.*, *193*(2), 101–110, doi:10.1016/S0048-9697(96)05325-9.

Carlson, T. N. (1981), Speculations on the movement of polluted air to the Arctic, *Atmos. Environ.*, *15*(8), 1473–1477, doi:10.1016/0004-6981(81)90354-1.

Claeys, M., W. Wang, R. Vermeylen, I. Kourtchev, X. Chi, Y. Farhat, J. D. Surratt, Y. Gómez-González, J. Sciare, and W. Maenhaut (2010), Chemical characterisation of marine aerosol at Amsterdam Island during the austral summer of 2006–2007, *J. Aerosol Sci.*, *41*(1), 13–22, doi:10.1016/j.jaerosci.2009.08.003.

Davidson, C. I., et al. (1993), Chemical constituents in the air and snow at Dye 3, Greenland—1. Seasonal variations, *Atmos. Environ., Part A*, *27*(17–18), 2709–2722.

DeCarlo, P. F., et al. (2006), Field-deployable, high-resolution, time-of-flight aerosol mass spectrometer, *Anal. Chem.*, *78*(24), 8281–8289, doi:10.1021/ac061249n.

DeCarlo, P. F., et al. (2008), Fast airborne aerosol size and chemistry measurements above Mexico City and central Mexico during the MILAGRO campaign, *Atmos. Chem. Phys.*, *8*(14), 4027–4048, doi:10.5194/acp-8-4027-2008.

Draxler, R. R., and G. D. Rolph (2003), HYSPLIT (HYbrid Single-Particle Lagrangian Integrated Trajectory), Air Resour. Lab., NOAA, Silver Spring, Md. (Available at http://www.arl.noaa.gov/ready/hysplit4.html.)

Farmer, D. K., A. Matsunaga, K. S. Docherty, J. D. Surratt, J. H. Seinfeld, P. J. Ziemann, and J. L. Jimenez (2010), Response of an aerosol mass spectrometer to organonitrates and organosulfates and implications for atmospheric chemistry, *Proc. Natl. Acad. Sci. U. S. A.*, *107*(15), 6670–6675, doi:10.1073/pnas.0912340107.

Ferek, R. J., P. V. Hobbs, L. F. Radke, J. A. Herring, W. T. Sturges, and G. F. Cota (1995), Dimethyl sulfide in the Arctic atmosphere, *J. Geophys. Res.*, *100*(D12), 26,093–26,104, doi:10.1029/95JD02374.

Gilardoni, S., S. Liu, S. Takahama, L. M. Russell, J. D. Allan, R. Steinbrecher, J. L. Jimenez, P. F. De Carlo, E. J. Dunlea, and D. Baumgardner (2009), Characterization of organic ambient aerosol during MIRAGE 2006 on three platforms, *Atmos. Chem. Phys.*, *9*(15), 5417–5432, doi:10.5194/acp-9-5417-2009.

Gómez-González, Y., et al. (2008), Characterization of organosulfates from the photooxidation of isoprene and unsaturated fatty acids in ambient aerosol using liquid chromatography/(−) electrospray ionization mass spectrometry, *J. Mass Spectrom.*, *43*(3), 371–382, doi:10.1002/jms.1329.

Greenaway, K. R. (1950), Experiences with Arctic flying weather, report, Can. Branch, R. Meteorol. Soc., Toronto, Ont., Canada.

Hawkins, L. N., L. M. Russell, D. S. Covert, P. K. Quinn, and T. S. Bates (2010), Carboxylic acids, sulfates, and organosulfates in processed continental organic aerosol over the southeast Pacific Ocean during VOCALS-REx 2008, *J. Geophys. Res.*, *115*, D13201, doi:10.1029/2009JD013276.

Hole, L. R., J. Christensen, M. Forsius, M. Nyman, A. Stohl, and S. Wilson (2006a), Sources of acidifying pollutants and Arctic haze precursors, in *AMAP Assessment Report: Acidifying Pollutants, Arctic Haze, and Acidification in the Arctic*, chap. 2, pp. 2–10, Arct. Monit. and Assess. Programme, Oslo.

Hole, L. R., J. Christensen, V. A. Ginzburg, V. Makarov, A. I. Polishok, T. Ruoho-Airola, and V. N. Vasilenko (2006b), Concentrations and deposition of acidifying air pollutants, in *AMAP Assessment Report: Acidifying Pollutants, Arctic Haze, and Acidification in the Arctic*, chap. 3, pp. 11–30, Arct. Monit. and Assess. Programme, Oslo.

Hole, L. R., J. H. Christensen, T. Ruoho-Airola, K. Tørseth, V. Ginzburg, and P. Glowacki (2009), Past and future trends in concentrations of sulphur and nitrogen compounds in the Arctic, *Atmos. Environ.*, *43*(4), 928–939, doi:10.1016/j.atmosenv.2008.10.043.

Huebert, B. J., and R. J. Charlson (2000), Uncertainties in data on organic aerosols, *Tellus, Ser. B*, *52*(5), 1249–1255, doi:10.1034/j.1600-0889.2000.01146.x.

Iinuma, Y., C. Müller, T. Berndt, O. Böge, M. Claeys, and H. Herrmann (2007), Evidence for the existence of organosulfates from β-pinene ozonolysis in ambient secondary organic aerosol, *Environ. Sci. Technol.*, *41*(19), 6678–6683, doi:10.1021/es070938t.

Iinuma, Y., O. Böge, A. Kahnt, and H. Herrmann (2009), Laboratory chamber studies on the formation of organosulfates from reactive uptake of monoterpene oxides, *Phys. Chem. Chem. Phys.*, *11*(36), 7985–7997, doi:10.1039/b904025k.

Isakson, J., T. A. Persson, and E. S. Lindgren (2001), Identification and assessment of ship emissions and their effects in the harbour of Göteborg, Sweden, *Atmos. Environ.*, *35*(21), 3659–3666, doi:10.1016/S1352-2310(00)00528-8.

Iversen, T. (1984), On the atmospheric transport of pollution to the Arctic, *Geophys. Res. Lett.*, *11*(5), 457–460, doi:10.1029/GL011i005p00457.

Iversen, T., and E. Joranger (1985), Arctic air pollution and large scale atmospheric flows, *Atmos. Environ.*, *19*(12), 2099–2108, doi:10.1016/0004-6981(85)90117-9.

Jayne, J. T., D. C. Leard, X. Zhang, P. Davidovits, K. A. Smith, C. E. Kolb, and D. R. Worsnop (2000), Development of an aerosol mass spectrometer for size and composition analysis of submicron particles, *Aerosol Sci. Technol.*, *33*(1), 49–70, doi:10.1080/027868200410840.

Jimenez, J. L., et al. (2009), Evolution of organic aerosols in the atmosphere, *Science*, *326*(5959), 1525–1529, doi:10.1126/science.1180353.

Lanz, V. A., M. R. Alfarra, U. Baltensperger, B. Buchmann, C. Hueglin, and A. S. H. Prévôt (2007), Source apportionment of submicron organic aerosols at an urban site by factor analytical modelling of aerosol mass spectra, *Atmos. Chem. Phys.*, *7*(6), 1503–1522, doi:10.5194/acp-7-1503-2007.

Lanz, V. A., S. Henne, J. Staehelin, C. Hueglin, M. K. Vollmer, M. Steinbacher, B. Buchmann, and S. Reimann (2009), Statistical analysis of anthropogenic non-methane VOC variability at a European background location (Jungfraujoch, Switzerland), *Atmos. Chem. Phys.*, *9*(10), 3445–3459, doi:10.5194/acp-9-3445-2009.

Law, K. S., and A. Stohl (2007), Arctic air pollution: Origins and impacts, *Science*, *315*(5818), 1537–1540, doi:10.1126/science.1137695.

Lerner, B. M., P. C. Murphy, and E. J. Williams (2009), Field measurements of small marine craft gaseous emission factors during NEAQS 2004 and TexAQS 2006, *Environ. Sci. Technol.*, *43*(21), 8213–8219, doi:10.1021/es901191p.

Li, S.-M., and L. A. Barrie (1993), Biogenic sulfur aerosol in the Arctic troposphere: 1. Contributions to total sulfate, *J. Geophys. Res.*, *98*(D11), 20,613–20,622, doi:10.1029/93JD02234.

Liggio, J., S.-M. Li, and R. McLaren (2005), Heterogeneous reactions of glyoxal on particulate matter: Identification of acetals and sulfate esters, *Environ. Sci. Technol.*, *39*(6), 1532–1541, doi:10.1021/es048375y.

Lim, Y. B., and P. J. Ziemann (2005), Products and mechanism of secondary organic aerosol formation from reactions of *n*-alkanes with OH radicals in the presence of NO_x, *Environ. Sci. Technol.*, *39*(23), 9229–9236, doi:10.1021/es051447g.

Lim, Y. B., and P. J. Ziemann (2009), Chemistry of secondary organic aerosol formation from OH radical-initiated reactions of linear, branched, and cyclic alkanes in the presence of NO_x, *Aerosol Sci. Technol.*, *43*(6), 604–619, doi:10.1080/02786820902802567.

Maria, S. F., L. M. Russell, B. J. Turpin, and R. J. Porcja (2002), FTIR measurements of functional groups and organic mass in aerosol samples over the Caribbean, *Atmos. Environ.*, *36*(33), 5185–5196, doi:10.1016/S1352-2310(02)00654-4.

Maria, S. F., L. M. Russell, B. J. Turpin, R. J. Porcja, T. L. Campos, R. J. Weber, and B. J. Huebert (2003), Source signatures of carbon monoxide and organic functional groups in Asian Pacific Regional Aerosol Characterization Experiment (ACE-Asia) submicron aerosol types, *J. Geophys. Res.*, *108*(D23), 8637, doi:10.1029/2003JD003703.

Maria, S. F., L. M. Russell, M. K. Gilles, and S. C. B. Myneni (2004), Organic aerosol growth mechanisms and their climate-forcing implications, *Science*, *306*(5703), 1921–1924, doi:10.1126/science.1103491.

Masclet, P., V. Hoyau, J. L. Jaffrezo, and H. Cachier (2000), Polycyclic aromatic hydrocarbon deposition on the ice sheet of Greenland, Part I: Superficial snow, *Atmos. Environ.*, *34*(19), 3195–3207, doi:10.1016/S1352-2310(99)00196-X.

Matthew, B. M., A. M. Middlebrook, and T. B. Onasch (2008), Collection efficiencies in an Aerodyne aerosol mass spectrometer as a function of particle phase for laboratory generated aerosols, *Aerosol Sci. Technol.*, *42*(11), 884–898, doi:10.1080/02786820802356797.

Mira-Salama, D., C. Grüning, N. R. Jensen, P. Cavalli, J.-P. Putaud, B. R. Larsen, F. Raes, and H. Coe (2008), Source attribution of urban smog episodes caused by coal combustion, *Atmos. Res.*, *88*(3–4), 294–304, doi:10.1016/j.atmosres.2007.11.025.

Mitchell, M. (1956), Visual range in the polar regions with particular reference to the Alaskan Arctic, *J. Atmos. Terr. Phys.*, spec. suppl., 195–211.

Ottar, B., J. M. Pacyna, and T. C. Berg (1986), Aircraft measurements of air pollution in the Norwegian Arctic, *Atmos. Environ.*, *20*(1), 87–100, doi:10.1016/0004-6981(86)90209-X.

Paatero, P. (1997), Least squares formulation of robust non-negative factor analysis, *Chemom. Intell. Lab. Syst.*, *37*(1), 23–35, doi:10.1016/S0169-7439(96)00044-5.

Paatero, P., and U. Tapper (1994), Positive matrix factorization: A non-negative factor model with optimal utilization of error estimates of data values, *Environmetrics*, *5*(2), 111–126, doi:10.1002/env.3170050203.

Pekney, N. J., C. I. Davidson, L. Zhou, and P. K. Hopke (2006), Application of PSCF and CPF to PMF-modeled sources of $PM_{2.5}$ in Pittsburgh, *Aerosol Sci. Technol.*, *40*(10), 952–961, doi:10.1080/02786820500543324.

Perri, M. J., Y. B. Lim, S. P. Seitzinger, and B. J. Turpin (2010), Organosulfates from glycolaldehyde in aqueous aerosols and clouds: Laboratory studies, *Atmos. Environ.*, *44*(21–22), 2658–2664, doi:10.1016/j.atmosenv.2010.03.031.

Polissar, A. V., P. Paatero, P. K. Hopke, W. C. Malm, and J. F. Sister (1998), Atmospheric aerosol over Alaska: 2. Elemental composition and sources, *J. Geophys. Res.*, *103*(D15), 19,045–19,057, doi:10.1029/98JD01212.

Polissar, A. V., P. K. Hopke, and J. M. Harris (2001), Source regions for atmospheric aerosol measured at Barrow, Alaska, *Environ. Sci. Technol.*, *35*(21), 4214–4226, doi:10.1021/es0107529.

Putaud, J.-P., et al. (2000), Chemical mass closure and assessment of the origin of the submicron aerosol in the marine boundary layer and the free troposphere at Tenerife during ACE-2, *Tellus, Ser. B*, *52*(2), 141–168, doi:10.1034/j.1600-0889.2000.00056.x.

Quinn, P. K., D. J. Coffman, V. N. Kapustin, T. S. Bates, and D. S. Covert (1998), Aerosol optical properties in the marine boundary layer during the First Aerosol Characterization Experiment (ACE 1) and the underlying chemical and physical aerosol properties, *J. Geophys. Res.*, *103*(D13), 16,547–16,563, doi:10.1029/97JD02345.

Quinn, P. K., et al. (2000), Surface submicron aerosol chemical composition: What fraction is not sulfate?, *J. Geophys. Res.*, *105*(D5), 6785–6805, doi:10.1029/1999JD901034.

Quinn, P. K., T. L. Miller, T. S. Bates, J. A. Ogren, E. Andrews, and G. E. Shaw (2002), A 3-year record of simultaneously measured aerosol chemical and optical properties at Barrow, Alaska, *J. Geophys. Res.*, *107*(D11), 4130, doi:10.1029/2001JD001248.

Quinn, P. K., et al. (2006), Impacts of sources and aging on submicrometer aerosol properties in the marine boundary layer across the Gulf of Maine, *J. Geophys. Res.*, *111*, D23S36, doi:10.1029/2006JD007582.

Quinn, P. K., G. E. Shaw, E. Andrews, E. G. Dutton, T. Ruoho-Airola, and S. L. Gong (2007), Arctic haze: Current trends and knowledge gaps, *Tellus, Ser. B*, *59*(1), 99–114, doi:10.1111/j.1600-0889.2006.00238.x.

Quinn, P. K., T. S. Bates, K. Schulz, and G. E. Shaw (2009), Decadal trends in aerosol chemical composition at Barrow, Alaska: 1976–2008, *Atmos. Chem. Phys.*, *9*(22), 8883–8888, doi:10.5194/acp-9-8883-2009.

Qureshi, S., V. A. Dutkiewicz, A. R. Khan, K. Swami, K. X. Yang, L. Husain, J. J. Schwab, and K. L. Demerjian (2006), Elemental composition of $PM_{2.5}$ aerosols in Queens, New York: Solubility and temporal trends, *Atmos. Environ.*, *40*, suppl. 2, 238–251, doi:10.1016/j.atmosenv.2005.12.070.

Rahn, K. A. (1981), The Mn/V ratio as a tracer of large-scale sources of pollution aerosol for the Arctic, *Atmos. Environ.*, *15*(8), 1457–1464, doi:10.1016/0004-6981(81)90352-8.

Rahn, K. A., and R. J. McCaffrey (1979), Compositional differences between Arctic aerosol and snow, *Nature*, *280*(5722), 479–480, doi:10.1038/280479a0.

Rahn, K. A., and R. J. McCaffrey (1980), On the origin and transport of the winter Arctic aerosol, *Ann. N. Y. Acad. Sci.*, *338*, 486–503, doi:10.1111/j.1749-6632.1980.tb17142.x.

Rahn, K. A., R. D. Borys, and G. E. Shaw (1977), The Asian source of Arctic haze bands, *Nature*, *268*(5622), 713–715, doi:10.1038/268713a0.

Rahn, K. A., D. H. Lowenthal, and J. M. Harris (1989), Long-range transport of pollution aerosol from Asia and the Arctic to Okushiri Island, Japan, *Atmos. Environ.*, *23*(11), 2597–2607, doi:10.1016/0004-6981(89)90268-0.

Ross, A. B., J. M. Jones, S. Chaiklangmuang, M. Pourkashanian, A. Williams, K. Kubica, J. T. Andersson, M. Kerst, P. Danihelka, and K. D. Bartle (2002), Measurement and prediction of the emission of pollutants from the combustion of coal and biomass in a fixed bed furnace, *Fuel*, *81*(5), 571–582, doi:10.1016/S0016-2361(01)00157-0.

Russell, L. M., S. Takahama, S. Liu, L. N. Hawkins, D. S. Covert, P. K. Quinn, and T. S. Bates (2009a), Oxygenated fraction and mass of organic aerosol from direct emission and atmospheric processing measured on the R/V *Ronald Brown* during TEXAQS/GoMACCS 2006, *J. Geophys. Res.*, *114*, D00F05, doi:10.1029/2008JD011275.

Russell, L. M., R. Bahadur, L. N. Hawkins, J. Allan, D. Baumgardner, P. K. Quinn, and T. S. Bates (2009b), Organic aerosol characterization by complementary measurements of chemical bonds and molecular fragments, *Atmos. Environ.*, *43*(38), 6100–6105, doi:10.1016/j.atmosenv.2009.09.036.

Russell, L. M., L. N. Hawkins, A. A. Frossard, P. K. Quinn, and T. S. Bates (2010), Carbohydrate-like composition of submicron atmospheric particles and their production from ocean bubble bursting, *Proc. Natl. Acad. Sci. U. S. A.*, *107*(15), 6652–6657, doi:10.1073/pnas.0908905107.

Russell, L. M., R. Bahadur, and P. J. Ziemann (2011), Identifying organic aerosol sources by comparing functional group composition in chamber and atmospheric particles, *Proc. Natl. Acad. Sci. U. S. A.*, doi:10.1073/pnas.1006461108, in press.

Sharma, M., and S. Maloo (2005), Assessment of ambient air PM_{10} and $PM_{2.5}$ and characterization of PM_{10} in the city of Kanpur, India, *Atmos. Environ.*, *39*(33), 6015–6026, doi:10.1016/j.atmosenv.2005.04.041.

Shaw, G. E. (1982), Evidence for a central Eurasian source area of Arctic haze in Alaska, *Nature*, *299*(5886), 815–818, doi:10.1038/299815a0.

Shaw, P. M., L. M. Russell, A. Jefferson, and P. K. Quinn (2010), Arctic organic aerosol measurements show particles from mixed combustion in spring haze and from frost flowers in winter, *Geophys. Res. Lett.*, *37*, L10803, doi:10.1029/2010GL042831.

Stohl, A. (2006), Characteristics of atmospheric transport into the Arctic troposphere, *J. Geophys. Res.*, *111*, D11306, doi:10.1029/2005JD006888.

Surratt, J. D., M. Lewandowski, J. H. Offenberg, M. Jaoui, T. E. Kleindienst, E. O. Edney, and J. H. Seinfeld (2007a), Effect of acidity on secondary organic aerosol formation from isoprene, *Environ. Sci. Technol.*, *41*(15), 5363–5369, doi:10.1021/es0704176.

Surratt, J. D., et al. (2007b), Evidence for organosulfates in secondary organic aerosol, *Environ. Sci. Technol.*, *41*(2), 517–527, doi:10.1021/es062081q.

Surratt, J. D., et al. (2008), Organosulfate formation in biogenic secondary organic aerosol, *J. Phys. Chem. A*, *112*(36), 8345–8378, doi:10.1021/jp802310p.

Surratt, J. D., A. W. H. Chan, N. C. Eddingsaas, M. Chan, C. L. Loza, A. J. Kwan, S. P. Hersey, R. C. Flagan, P. O. Wennberg, and J. H. Seinfeld (2010), Reactive intermediates revealed in secondary organic aerosol formation from isoprene, *Proc. Natl. Acad. Sci. U. S. A.*, *107*(15), 6640–6645, doi:10.1073/pnas.0911114107.

Takegawa, N., T. Miyakawa, K. Kawamura, and Y. Kondo (2007), Contribution of selected dicarboxylic and ω-oxocarboxylic acids in ambient aerosol to the m/z 44 signal of an Aerodyne aerosol mass spectrometer, *Aerosol Sci. Technol.*, *41*, 418–437, doi:10.1080/02786820701203215.

Tzimas, E., A. Georgakaki, and S. D. Peteves (2009), *Future Fossil Fuel Electricity Generation in Europe: Options and Consequences*, Inst. for Energy, Joint Res. Cent., Luxembourg.

Ulbrich, I. M., M. R. Canagaratna, Q. Zhang, D. R. Worsnop, and J. L. Jimenez (2009), Interpretation of organic components from Positive Matrix Factorization of aerosol mass spectrometric data, *Atmos. Chem. Phys.*, *9*(9), 2891–2918, doi:10.5194/acp-9-2891-2009.

U.S. Department of Agriculture (2010), Fire and aviation management fiscal year 2009 accountability report, 54 pp., U.S. Forest Service, Washington, D. C.

Warneke, C., et al. (2009), Biomass burning in Siberia and Kazakhstan as an important source for haze over the Alaskan Arctic in April 2008, *Geophys. Res. Lett.*, *36*, L02813, doi:10.1029/2008GL036194.

Weiler, K., H. Fischer, D. Fritzsche, U. Ruth, F. Wilhelms, and H. Miller (2005), Glaciochemical reconnaissance of a new ice core from Severnya Zemlya, Eurasian Arctic, *J. Glaciol.*, *51*(172), 64–74, doi:10.3189/172756505781829629.

Zhang, Q., D. R. Worsnop, M. R. Canagaratna, and J. L. Jimenez (2005a), Hydrocarbon-like and oxygenated organic aerosols in Pittsburgh: Insights into sources and processes of organic aerosols, *Atmos. Chem. Phys.*, *5*, 3289–3311, doi:10.5194/acp-5-3289-2005.

Zhang, Q., M. R. Alfarra, D. R. Worsnop, J. D. Allan, H. Coe, M. R. Canagaratna, and J. L. Jimenez (2005b), Deconvolution and quantification of hydrocarbon-like and oxygenated organic aerosols based on aerosol mass spectrometry, *Environ. Sci. Technol.*, *39*(13), 4938–4952, doi:10.1021/es048568l.

T. S. Bates and P. K. Quinn, Pacific Marine Environmental Laboratory, NOAA, 7600 Sand Point Way NE, Seattle, WA 98115, USA.

M. R. Canagaratna and D. R. Worsnop, Aerodyne Research, Inc., 45 Manning Rd., Billerica, MA 01821, USA.

A. A. Frossard, L. M. Russell, and P. M. Shaw, Scripps Institution of Oceanography, University of California, San Diego, Mail Code 0221, 9500 Gilman Dr., La Jolla, CA 92093, USA. (lmrussell@ucsd.edu)

J. H. Kroll, Department of Civil and Environmental Engineering, Massachusetts Institute of Technology, Cambridge, MA 02139, USA.